

Visualization of Sinusoidal and Varicose Instabilities of Streaks in a Boundary Layer

Chernoray, V. G.*¹, Kozlov, V. V.*², Löfdahl, L.*¹ and Chun, H. H.*³

*1 Applied Mechanics, Chalmers University of Technology, SE-412 96, Gothenburg, Sweden.

*2 Institute of Theoretical and Applied Mechanics SB RAS, 630090, Novosibirsk, Russia.

E-mail: kozlov@itam.nsc.ru

*3 Naval Architecture & Ocean Engineering, Pusan National University, 609-735, Pusan, Korea.

Received 17 February 2006
Revised 25 April 2006

Abstract : Nonlinear instabilities of boundary layer streaks are investigated experimentally. Extensive measurements visualizing the sinusoidal and varicose instabilities of streaky structures at nonlinear stage of the breakdown process in boundary layer are presented. The flow behaviour in the course of spatial evolution of the streaky structures with a secondary high-frequency disturbance generated on them is discussed. Various scenarios of origination and development of coherent vortex structures examined in physical experiments are considered. Specific features of the development of sinusoidal and varicose cases of destruction of the steady streamwise streaks are demonstrated, such as transverse and streamwise modulations of the streak by the secondary-disturbance frequency, appearance of new streaky structures in the downstream direction, and emergence and evolution of unsteady Λ -shaped structures localized in space in both cases.

Keywords : Visualization, Hot-wire anemometry, Sinusoidal and Varicose instabilities, Streaks.

1. Introduction

Laminar-turbulent transition in boundary layers is routed in many instances through the transverse modulation of the layer by steady (e.g. Görtler vortices, crossflow vortices on swept wings) and unsteady (streaky structures in the case of high free-stream turbulence, Λ -, Ω -, and hairpin vortices) streamwise flow perturbations. The origination and evolution of the mentioned disturbances has been studied in numerous experimental and numerical researches (see Haidary and Smith, 1994; Panton, 2001; Winoto et al., 2005; Zharkova et al., 2002). The streamwise structures have been also found in the turbulent boundary layers about 50 years ago (Panton, 2001), and their role in the regeneration of turbulent oscillations has been extensively examined since that time.

Transverse modulations of the wall-bounded flows by the streamwise structures generate conditions for the origination and development of secondary oscillations, which downstream evolution leads to the boundary-layer turbulization. For example, visualizations of the flow modulated by the Görtler vortices (Bippes, 1972; Ito, 1985) showed that transition in this flow is determined by the secondary mechanisms, which produce independent instability waves on each vortex pair so that the neighbouring pairs can amplify a secondary motion of different type, either in the form of periodic meandering of vortices in the transverse direction or in the form of horse-shoe bunches in the region of strong transverse shear. These phenomena are referred to as the sinusoidal and varicose modes of instability, respectively. Sometimes they are compared with the odd and even modes known from the analytical and numerical analyses of the secondary instability of Görtler vortices.

The reason for the secondary instability is an inviscid local mechanism caused by the inflections in the instantaneous velocity profiles both in the wall-normal (varicose mode) and in the transverse (sinusoidal mode) directions. The choice of the instability mode excited first and growing most rapidly depends on the initial conditions, in particular, on a distance between the streamwise disturbances. It was found numerically (Bottaro and Klingmann, 1996) that the varicose mode dominates in long-wave vortices, whereas the sinusoidal mode prevails in short-wave vortices which are more frequently encountered. The primary reason is that the vortices with a large wavelength induce a weak transverse shear and the vortices with a short wavelength - a strong one. Direct numerical simulations of the varicose instability in a turbulent boundary layer (Skote et al., 2002) revealed that the horse-shoe vortices generated in laminar and turbulent boundary layers are very similar. Also, it was found that the mechanisms of the generation of horse-shoe vortices in turbulent boundary layers are related to the inflectional instability of the streaky structures. The horse-shoe vortices can induce new streaky structures in the viscous sublayer of turbulent boundary layer, which agrees with the results of Adrian et al. (2000). On the other hand, the sinusoidal instability associated with the inflectional transverse velocity profiles has been confirmed in other studies (Kawahara et al., 1998; Schoppa and Hussain, 1997). One expects that both instability types are important mechanisms of turbulence self-sustain in turbulent boundary layers: the sinusoidal one serves to regenerate the near-wall turbulence (Hamilton et al., 1995; Brandt and Henningson, 2002), and the varicose instability is responsible for the generation of horse-shoe vortices occupying the flow region farther from the wall (Haidary and Smith, 1994; Adrian et al., 2000; Skote et al., 2002; Robinson, 1991).

Present paper deals with the varicose and sinusoidal instabilities of the streamwise streaks in the Blasius flow which is important for understanding of the mechanisms of laminar-turbulent transition and turbulence regeneration in boundary layers. The main attention is paid to the coherent structures arising due to the streak instabilities. In contrast to similar experiments of Asai et al. (2002) and Konishi and Asai (2004) the study is performed in more detail with emphasis on the nonlinear development of the boundary layer perturbations.

2. Experimental Setup and Measurement Procedure

Experimental method used in this study is hot-wire visualization which is especially suitable for studies of three-dimensional transition processes in complex wall-bounded flows. A comprehensive system for automated traversing and data acquisition has been designed and developed for this task at Chalmers University of Technology. Hot-wire readings within the boundary layer are recorded in a three-dimensional (3D) mesh over the surface of the model. At each point the phase-locked traces are sampled and ensemble averaged over a period of the boundary-layer oscillation. These are, then, assembled to form a four-dimensional spatial and temporal matrix. The waveforms are separated into the discrete scans of which they consist and, in this fashion, a number of 3D 'frame' matrices are obtained. Isosurfaces of fluctuating velocity are plotted for each frame and displayed in sequence to obtain a dynamic visualization of the process.

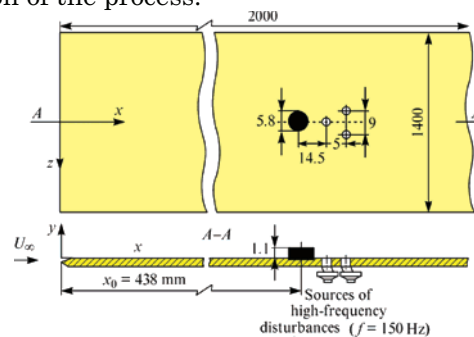


Fig. 1. Layout of the experiment.

Experiments were performed in a subsonic low-turbulent wind tunnel on a flat plate model (Fig. 1). The plate has an elliptic form of the leading edge with the axes ratio of 12:1. The flow velocity U_∞ was 7.8 m/s and the flow turbulence level was well below 0.1 %. A boundary layer streak was generated by a cylindrical roughness element of 1.1 mm height and 5.8 mm in diameter placed in the centre of the model at a distance of 438 mm from its leading edge. The height of the element was

comparable with the local boundary-layer displacement thickness δ^* , which was 1.5 mm. The Reynolds number was equal to $R^* = \delta^* U_\infty / \nu = 780$ for $x = x_0$. On the smooth plate, in the absence of the streak generator, the laminar boundary layer was developed in the region of measurements with the mean velocity profile close to the Blasius one. In what follows, the coordinate axes are directed downstream (x), normal to the surface (y), and in the transverse direction (z); the position of the roughness element $x = 438$ mm is marked by x_0 .

The streaky structure instability was controlled by the periodic artificial disturbances injected in the boundary layer through three orifices 3 mm in diameter. One of them arranged at $x - x_0 = 14.5$ mm and $z = 0$ was used to excite the symmetric oscillations of the streak, and two others to generate the antisymmetric disturbances. The orifices were separately connected to three loudspeakers by vinyl tubes, and the antisymmetric perturbations were excited by the sinusoidal signals in antiphase. The excitation frequency of the secondary disturbances was $f = 150$ Hz, and corresponding nondimensional value is $2\pi f \nu / U_\infty^2 \times 10^6 = 232$. The frequency was chosen close to that of the disturbances most rapidly growing under the natural conditions. Amplitude of the secondary disturbances reached 10 % of U_∞ near the source making it possible to study the nonlinear stage of breakdown which was of the primary interest.

The hot-wire anemometer measured the streamwise velocity component u . The hot-wire probe was equipped with a gold-plated tungsten wire of 1.2 mm active length and 5 μm in diameter. The maximum error in the probe calibration was within 1% for all calibration points. All measurements were performed in an automated mode with use of a traversing system moving the probe in a 3D space by a specially developed software involving LabVIEW. Approximately 10^4 spatial points were mapped in each case.

Data reduction and visualization is performed using the MatLab software package. The measured voltage traces were converted into the velocity traces and then phase averaged over 100 disturbance periods to form a matrix $u_{ave}(x, y, z, t)$. This velocity is decomposed into a mean U and fluctuation \tilde{u} components such that $u_{ave} = U + \tilde{u}$. Subtraction of the base undisturbed flow U_B gives the total disturbance velocity $u_{tot} = u_{ave} - U_B$.

3. Results and Discussion

3.1 Velocity Field Downstream of the Roughness Element

The contour diagrams of the streamwise velocity fluctuations in Fig. 2 provide an idea about the structure of the secondary high-frequency disturbances of the sinusoidal and varicose types near the roughness element. The distribution of the sinusoidal perturbations (Fig. 2(a)) is symmetric with respect to $z = 0$, while its phase is subject to a 180-degree jump across the symmetry axis; thus, the amplitude of this mode vanishes at $z = 0$. Vice versa, the distribution of the varicose mode (Fig. 2(b)) displays the maximum amplitude at $z = 0$ and the absence of the transverse jump in phase. The oscillations excited can be identified as the inherent modes of a three-dimensional shear layer related to the streaky structure. Despite a clearly nonlinear character of the excited waves even near their source, the distributions in Fig. 2 correlate very well with similar data of Asai et. al. (2002). The phase velocities of the symmetric and antisymmetric modes are close to the local flow velocities at the profile inflection points along the z and y axis, respectively. The velocity gradients $\partial U / \partial z$ and $\partial U / \partial y$ attain the highest values at these inflection points.

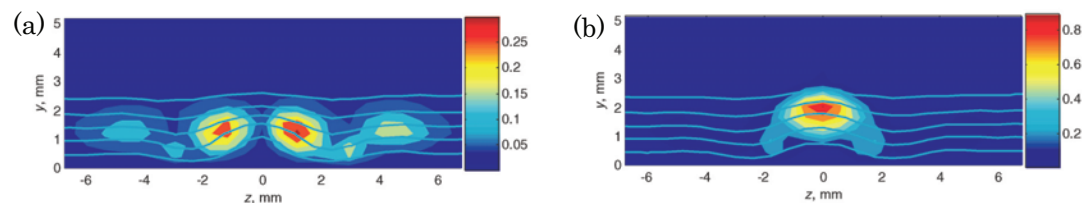


Fig. 2. Disturbances near the roughness element, at $x - x_0 = 30$ mm for (a) sinusoidal and (b) varicose types of instability. Filled contours show r.m.s. amplitude of the secondary high-frequency disturbances (\tilde{u} in m/s). Lines depict contours of mean velocity at levels of 15, 30 ... 75 % of U_∞ .

3.2 Origination of Coherent Structures at Nonlinear Development of the Sinusoidal and Varicose Modes of Instability

Figures 3 to 7 show the streamwise evolution of the streak affected by the secondary oscillations. The growth of the high-frequency secondary disturbance amplitudes \tilde{u} in the downstream direction in the range of $x-x_0$ from 30 to 150 mm was not very high, namely, disturbance amplitude increased from 4 to 16 % of U_∞ for the sinusoidal mode and from 12 to 17 % of U_∞ for the varicose mode. Whereas the influence of the disturbances on the mean flow was significant, and corresponding distortions of the base flow were observed from 15 to 32 % of U_∞ for the sinusoidal mode and from 10 to 32 % of U_∞ for the varicose one. The influence of the sinusoidal perturbations is particularly strong: it exerts a powerful effect on the mean flow at a relatively small initial amplitude of the secondary disturbance. This supports the conclusions of many researchers that the sinusoidal instability is more 'dangerous'.

Considering the initial development of the antisymmetric mode in more detail (Fig. 3(a)) it can be noted that the time-periodic part of the perturbation \tilde{u} is composed of two rows of Λ -shaped structures. It is clearly seen that the disturbance is perfectly antisymmetric during this phase of the development, and this behaviour is remarkable for the strongly nonlinear disturbance. On the other hand, it can be observed in Fig 3(b) that a gradual change of the disturbance amplitude distribution occurs as disturbance develops downstream. This happens owing to the interaction with the mean flow and this effect is a direct consequence of the disturbance nonlinearity.

The antisymmetric sinusoidal mode leads to the meandering of the streaky structure over a half-period by 180° , see Fig. 4. This figure shows isosurfaces of the total instantaneous flow perturbation at different levels. As is seen, with streak breakdown evolving downstream the multiplication of streaky structures and appearance of the coherent structures such as Λ -vortices takes place. A similar process is also observed in the case of the development of the varicose instability (see Fig. 6). However, the symmetry of the perturbation is different in the latter case. As Fig. 6 demonstrates, at initial stage of the spatial development the periodic pinching of the streaky structure occurs and further downstream the hot-wire measurements reveal a multiplication of the streaky structures and emergence of additional coherent structures. It can be noted that the latter phenomenon was not observed in previous experimental works (Asai et. al., 2002), since the nonlinear stage of the development of both types of instabilities was examined only at initial stage and with less detailed hot-wire measurements than those used in the present study.

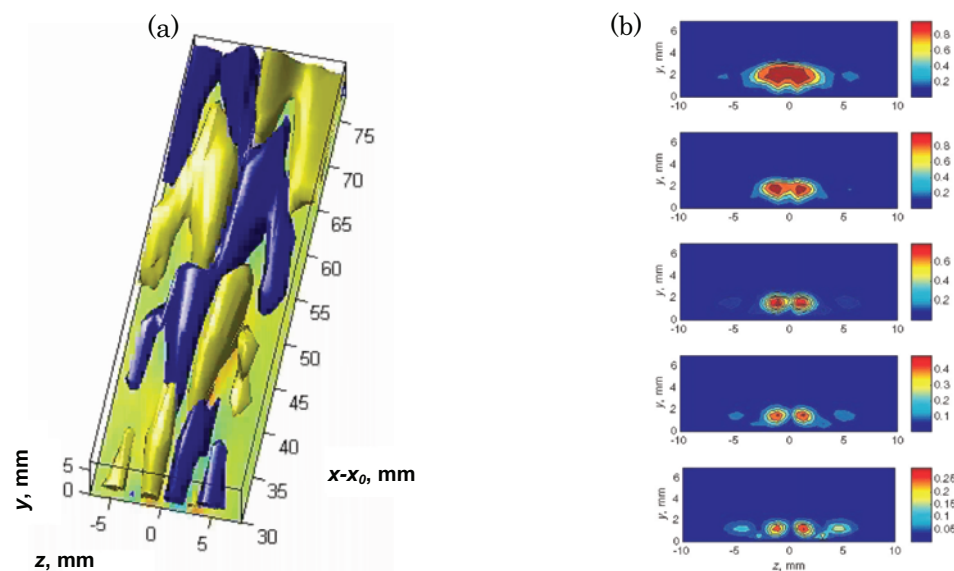


Fig. 3. Initial development of the sinusoidal instability mode. (a) isosurfaces of the instantaneous time-periodic velocity ($\tilde{u}/U_\infty = 0.75\%$, yellow; $\tilde{u}/U_\infty = -0.75\%$, blue); (b) contours of r.m.s. velocity amplitude at streamwise stations 30, 42, 54, 66 and 78 mm, increasing from bottom to top.

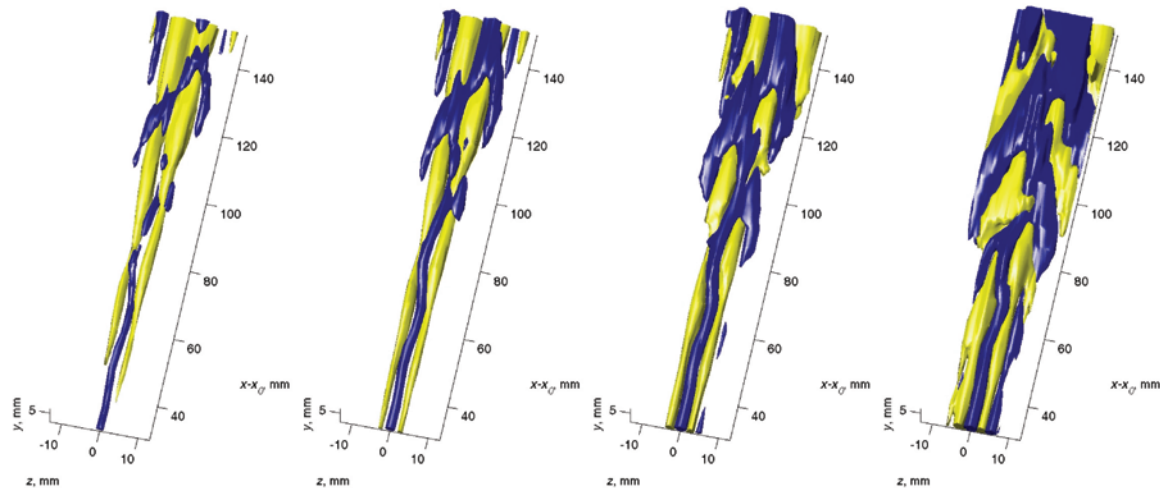


Fig. 4. Streak breakdown through the sinusoidal instability. Isosurfaces of total instantaneous flow perturbation u_{tot} (yellow – positive, blue – negative) at different levels: $\pm 10.3\%$, $\pm 6.4\%$, $\pm 2.6\%$, and $\pm 0.65\%$ of U_∞ , from left to right.

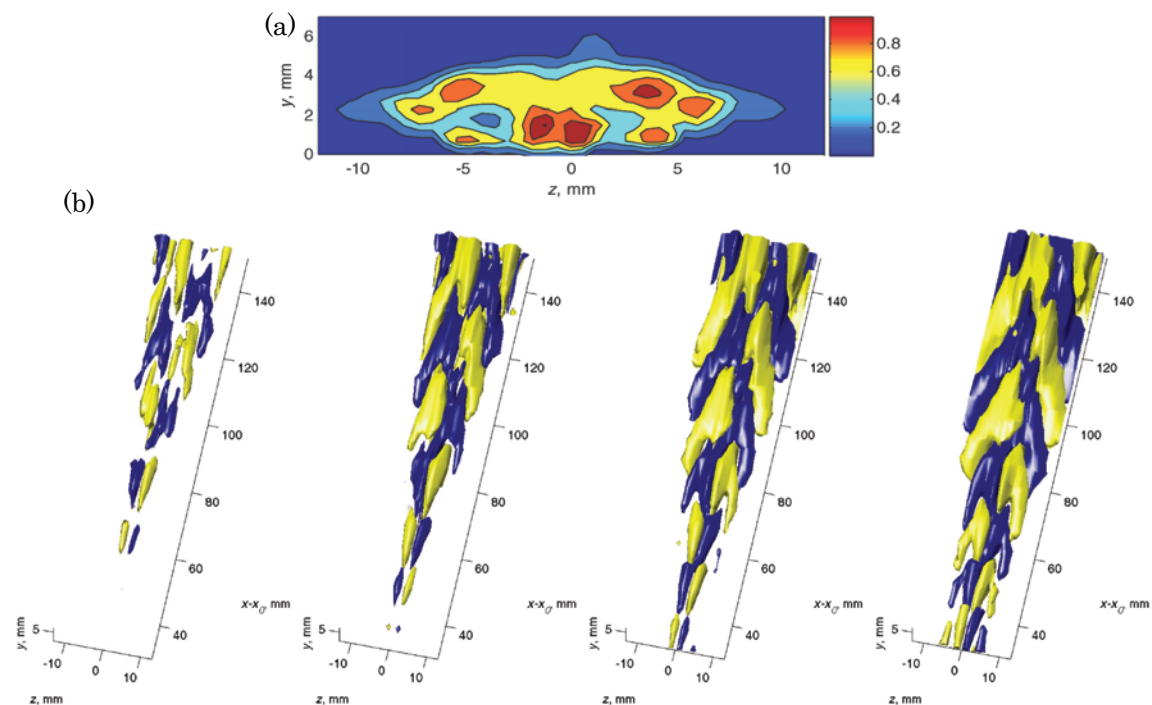


Fig. 5. Spatial patterns of the development of high-frequency disturbance of the sinusoidal instability. (a) contours of r.m.s. velocity amplitude at $x - x_0 = 114$ mm; (b) isosurfaces of time-periodic velocity \tilde{u} : $\pm 6.4\%$, 2.6% , 1.3% , and 0.65% of U_∞ , from left to right.

In Fig. 4 the sinusoidal destruction of the streaky structure is shown by the isosurface diagrams of total instantaneous flow perturbation u_{tot} . A very typical for the sinusoidal mode streak meandering is visualized during the initial stage of breakdown and further downstream the structure of the disturbed region is transformed into the coherent structures which resemble the Λ -vortices. The transverse smearing of the disturbed flow region in the downstream direction is observed very clearly and our analysis shows that this phenomenon is associated with the multiplication of the streaky structures (generation of new streaky structures). In given diagrams this process is evidenced by the appearance of new closed regions of isolines at $x - x_0 = 140$ mm. The development of the secondary high-frequency disturbance in Fig. 5 demonstrates the transverse

fragmentation of initially well-defined and 'simple' secondary perturbations into a number of closed regions of isolines near the wall. The streak oscillations (meandering) lead to the generation of a chain of streamwise vortices entrained downstream with a transverse multiplication of these vortices. At the initial stage of the disturbance evolution one can observe a pair of streamwise velocity deformations of alternating sign which are transformed further downstream into the Λ -shaped structures; and the transverse scale of these coherent structures increases thereby. In a flow pattern with the levels of disturbance amplitude of $\pm 6.4\% U_\infty$ (Fig. 5, leftmost), one can mainly observe quasi-streamwise structures, whereas in the case of the spatial pattern with the disturbance amplitudes of $\pm 0.65\% U_\infty$ (Fig. 5, rightmost), one can see typical coherent structures similar to the Λ -vortices. Thus, the detailed hot-wire measurements of the nonlinear stage of the sinusoidal instability showed that the secondary high-frequency destruction of the streaky structure is associated with the formation of Λ -structures whose downstream evolution leads to the flow turbulization.

For the varicose mode, the isosurface diagrams of the total instantaneous flow perturbation (Fig. 6) also demonstrate the transverse smearing of the disturbed region in the downstream direction, which is related to the multiplication of streaky structures. This is evidenced by the emergence of new closed regions of isolines at $x - x_0 = 80$ and 100 mm. The spatial pattern of the disturbance evolution shows that the streamwise modulation in the form of streak bunching is observed at the initial part, which is typical for the development of the varicose instability. Further downstream, however, the structure of the disturbed region is transformed into typical coherent structures resembling Λ -vortices, as in the case of the sinusoidal streak destruction. In contrast to the previous case, three rows of the Λ -structures can be seen. On the sides the Λ -structures are asymmetric, i.e. the second 'leg' is at the stage of formation. Furthermore, the secondary high-frequency disturbance generated on the streaky structure (Fig. 7) reveals the symmetric Λ -shapes located on the centreline. These are formed from a sequence of the periodical structures. The process of development of the secondary disturbance is particularly well seen in this spatial picture with different amplitude levels. These diagrams demonstrate transverse fragmentation of the initially well-defined structure in the downstream direction into a series of elongated regions, as in the case with the sinusoidal instability. The streamwise modulation of the streak leads to the generation of hairpin vortices or a pair of counter-rotating quasi-streamwise vortices in the region of $z = \pm 5$ mm. On the transverse boundaries of the disturbed region, the Λ -structures or hairpin vortices appear to be asymmetric; nevertheless, the second counter-rotating 'leg' of these coherent structures can be observed clearly as forming. Thus, the transverse multiplication of the longitudinal structures takes place. It can be deduced that the low-velocity fluid is moving upward there, and each leg of the hairpin vortex evolves into a pair of counter-rotating streamwise vortices on each period of the secondary disturbance. The spatial pattern of disturbance amplitude levels of $\pm 2.6\%$ of U_∞ is visualizing localized structures modulating the low-speed streak, which are multiplied in transverse direction with emergence of Λ -vortices. The flow pattern at the level of the disturbance amplitude of $\pm 0.4\% U_\infty$ shows the origination of Λ -vortices at a significantly earlier stage.

Finally, we note that the nonlinear stage of the 'classical' scenario of the laminar-turbulent transition is associated with a three-dimensional distortion of the two-dimensional Tollmien-Schlichting waves and the formation of three-dimensional coherent structures such as Λ -vortices. Present investigation showed that there are other scenarios of the Λ -structure origination in the near-wall shear flows, in particular in the process of the secondary high-frequency instability of streaks of the sinusoidal and varicose types. This result is important both for understanding the mechanisms of turbulization of flows modulated by the streaky structures and for understanding the mechanisms of the turbulence reproduction in turbulent flows, where the dynamics of the coherent structures of the viscous sublayer plays an important role. This also means that both modes of the streak instability may contribute to the formation of the horse-shoe vortices in the outer part of turbulent boundary layers. On the other hand, various methods are known for controlling the development of coherent structures such as Λ -vortices and hairpin vortices and can be used to control both sinusoidal and varicose instability modes.

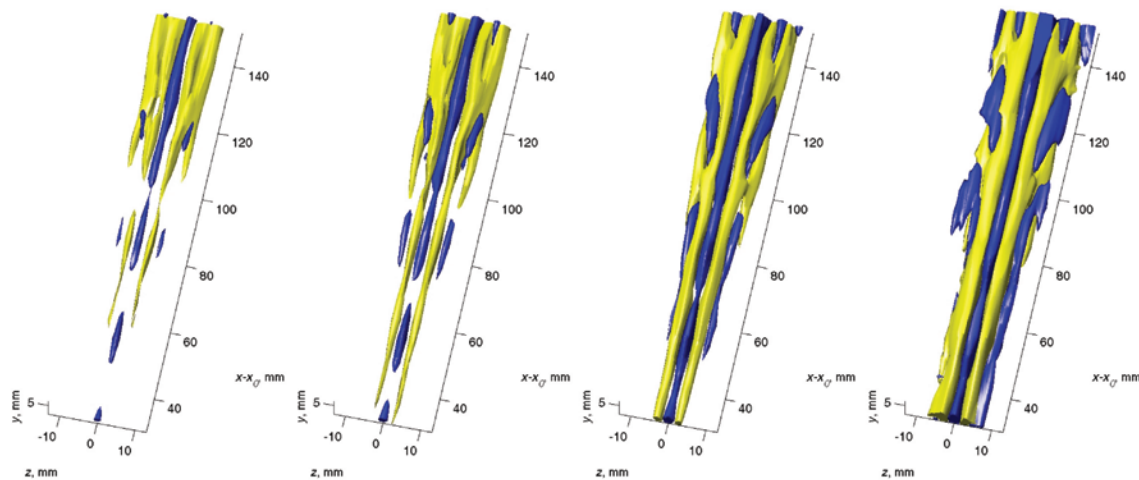


Fig. 6. Patterns of the varicose destruction of the streaky structure. Isosurfaces of total instantaneous flow perturbation u_{tot} (yellow – positive, blue – negative) at different levels: $\pm 10.3\%$, 6.4% , 2.6% , and 0.65% of U_∞ , from left to right.

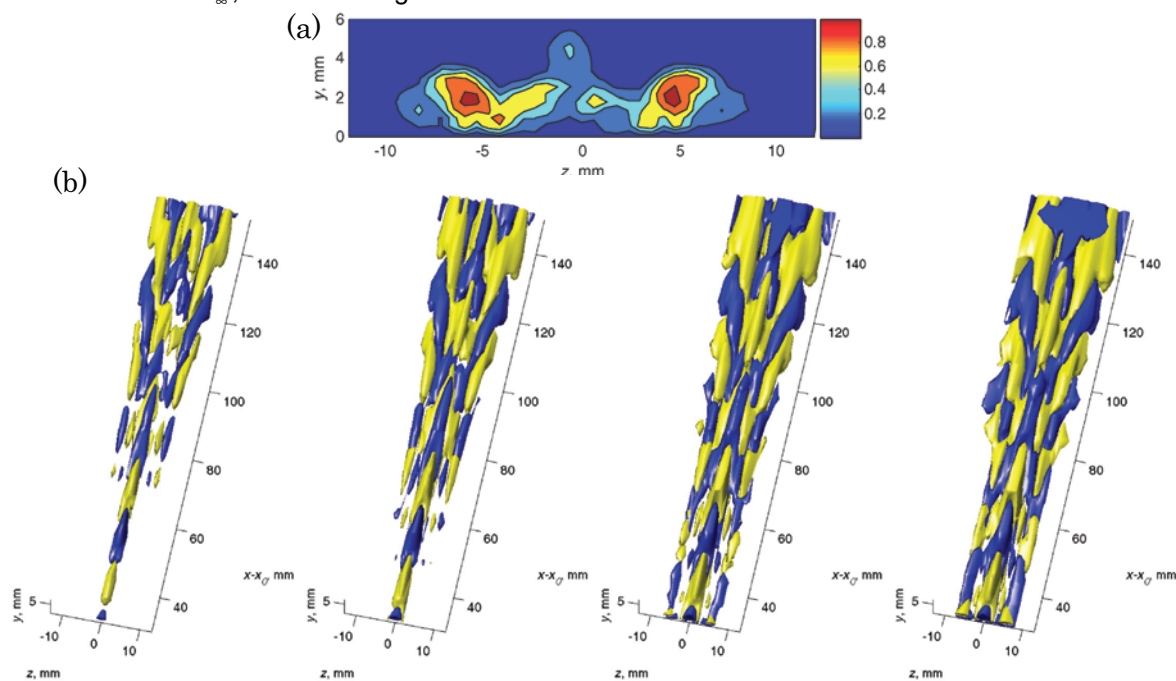


Fig. 7. Spatial patterns of the development of high-frequency disturbance of the varicose instability. (a) contours of r.m.s. velocity amplitude at $x - x_0 = 114$ mm; (b) isosurfaces of time-periodic velocity \tilde{u} : $\pm 2.6\%$, 1.3% , 0.65% , 0.4% of U_∞ , from left to right.

3. Conclusions

Streak secondary high-frequency instabilities of sinusoidal and varicose types at the nonlinear stage of their development lead to the dispersion of the disturbed regions via the process of multiplication of the streaky structures. The mechanism of the nonlinear streak destruction by means of the development of the secondary disturbances is related to the formation of coherent structures resembling Λ -vortices (or horse-shoe vortices) for both sinusoidal and varicose modes of instability. It is shown that in both these cases the Λ -vortices multiply in the transverse direction in the course of the downstream evolution and move upward propagating into the external part of the boundary layer.

Acknowledgments

This work was supported by the Ministry of Education and Science of the Russian Federation, grant

No. RNP.2.1.2.3370, the ERC program (Advanced Ship Engineering Research Center) of MOST/KOSEF, grant No. R11-2002-104-05001-0, and the Korea Research Foundation grant funded by the Korea Government (MOEHRD), grant No. KRF-2005-212-D00024.

References

- Adrian, R. J., Meinhart, C. D. and Tomkins, C. D., Vortex organization in the outer region of the turbulent boundary layer, *J. Fluid Mech.*, 422 (2000), 1-23.
- Asai, M., Minagawa, M. and Nishioka, M., The stability and breakdown of near-wall low-speed streak, *J. Fluid Mech.*, 455 (2002), 289-314.
- Bippes, H., Experimentelle Untersuchung des laminar-turbulenten Umschlags an einer parallel angestromten konkaven Wand, *Sitzungsberichte der Heidelberger Akademie der Wissenschaften Mathematisch-naturwissenschaftliche Klasse*, Jahrgang, 3 (1972) Abhandlung, 103-180. (also NASA-TM-72243, March 1978).
- Bottaro, A. and Klingmann, B. G. B., On the linear breakdown of Görtler vortices, *Eur. J. Mech. B-Fluids*, 15 (1996), 301-330.
- Brandt, L. and Henningson, D. S., Transition of streamwise streaks in zero-pressure-gradient boundary layers, *J. Fluid Mech.*, 472 (2002), 229-261.
- Haidary, H. A. and Smith, C. R., The generation and regeneration of single hairpin vortices, *J. Fluid Mech.*, 227 (1994) 135-151.
- Hamilton, H., Kim, J. and Waleffe, F., Regeneration of near-wall turbulence structures, *J. Fluid Mech.*, 287 (1995), 317-348.
- Ito, A., Breakdown structure of longitudinal vortices along a concave wall, *J. Japan Soc. Aerosp. Sci.*, 33 (1985), 166-173.
- Kawahara, G., Jimenez, J., Uhlmann, M. and Pinelli, A., The instability of streaks in near-wall turbulence: Center for Turbulence Research, Annual Research Briefs (1998), 155-170.
- Konishi, Y. and Asai, M., Experimental investigation of the instability of spanwise-periodic low-speed streaks, *Fluid Dyn. Res.*, 34 (2004), 299-315.
- Panton, R. L., Overview of the self-sustaining mechanisms of wall turbulence, *Prog. Aerosp. Sci.*, 37 (2001), 341-383.
- Robinson, S. K., The kinematics of turbulent boundary layer structure, (1991) NASA TM 103859.
- Schoppa, W. and Hussain, F., Genesis and dynamics of coherent structures in near-wall turbulence: A new look, *Self-sustaining Mechanisms of Wall Turbulence*, R. L. Panton (ed.), Computational mechanics, (1997), Southampton.
- Skote, M., Haritonidis, J. H. and Henningson, D.S., Varicose instabilities in turbulent boundary layers, *Phys. Fluids*, 4-7 (2002), 2309-2323.
- Winoto, S. H., Mitsudharmadi, H. and Shah, D. A., Visualizing Görtler vortices, *J. Vis.*, 8-4 (2005), 315-322.
- Zharkova, G. M., Zanin, B. Y., Kovrizhina, V. N. and Brylyakov, A. P., Free stream turbulence effect on the flow structure over the finite span straight wing, *J. Vis.*, 5-2 (2002), 169-176.

Author Profile



Valery G. Chernoray: He received his Ph.D. in Physics-Mathematics in 2002 from the Institute of Theoretical and Applied Mechanics of Russian Academy of Sciences. He worked as a full-time research fellow in the Institute of Theoretical and Applied Mechanics. He works in the department of Applied Mechanics at Chalmers University of Technology in Gothenburg, Sweden as an assistant professor since 2005. In August 16, 2004 he was awarded the Top National Prize in Science (State Prize of Russian Federation), which was given for outstanding work in science. His current research interests are transitional and turbulent flows, and various techniques of flow control.



Victor V. Kozlov: He is a Head of Laboratory of Aero-Physics Researches at ITAM, Novosibirsk, Russia, Professor at the Novosibirsk State University. He obtained his Ph.D. in Physics-Mathematics from the Institute of Theoretical and Applied Mechanics of Russian Academy of Sciences in 1976 and defended his Academic Professor's Thesis in 1987. He was awarded the Silver Zhukovsky Medal for great contribution to the aviation theory from the Russian Academy of Sciences in 1993. His main research interests are the experimental studies of flow stability and transition to turbulence.



Lennart Löfdahl: He is a Professor in Fluid Dynamics and adviser for graduate students at Chalmers University of Technology in Gothenburg, Sweden since 1995. He received his Doctoral degree from Chalmers University of Technology in 1982 and Docent degree in 1984. His research interests include: MEMS devices in fluid mechanics application, study of turbulence and turbulence modelling and heat transfer, as well as ground vehicle aerodynamics.



Ho Hwan Chun: He is a Professor in the Department of Naval Architecture & Ocean Engineering and director of Advanced Ship Engineering Research Center (ASERC). He obtained his Ph.D from University of Glasgow, UK., in 1988. His research interests include: ship hydrodynamics, computational fluid dynamics, high speed ship designs, towing tankery problems, fluid mechanics and drag reduction.